

Composition Control of YSZ Thin Film Prepared by MOCVD

Tomokazu Matsuzaki*, Norikazu Okuda, Kazuo Shinozaki, Nobuyasu Mizutani and Hiroshi Funakubo*

Department of Inorganic Materials, Faculty of Engineering, Tokyo Institute of Technology, 2-12-1, Ookayama, Meguro-ku, Tokyo 152-8552, Japan

*Department of Innovative and Engineered Materials, Interdisciplinary Graduated School of Science and Engineering, Tokyo Institute of Technology, 4259 Nagatsuta-cho, Midori-ku, Yokohama 226-8502, Japan

(Received September 23, 1998)

Zirconia films stabilized by Y_2O_3 , YSZ, films were deposited by metal organic chemical vapor deposition (MOCVD) onto various kind of substrates. Y_2O_3 , ZrO_2 and the mixtures of these two were deposited and characterized. The deposition rate, the film composition and the structure could be systematically varied through the $Y(C_{11}H_{19}O_2)_3$, $Zr(O-t-C_4H_9)_4$ source gas ratios and the deposition temperature. The Y/Zr ratio in YSZ film could be adjusted by controlling the ratio of $Y(C_{11}H_{19}O_2)_3$ to $Zr(O-t-C_4H_9)_4$ partial pressures. This is because the ratios of the deposition rates of Y and Zr atoms in Y_2O_3 and ZrO_2 films to those in YSZ films, Φ , are constant irrespective of the input gas concentration. However, the Y/Zr ratio was found to be smaller than that estimated based on the deposition rates of un-mixed Y_2O_3 and ZrO_2 films. This is because the Φ s of Y and Zr atoms are not equal. The activation energy of Y_2O_3 component in YSZ films was similar to that of ZrO_2 component in YSZ films. These YSZ values were more than 4 times larger than those of un-mixed Y_2O_3 or ZrO_2 films.

Key words: YSZ, MOCVD, Deposition mechanism, Activation energy, Deposition rate

I. Introduction

Metal organic chemical vapor deposition (MOCVD) is known to offer excellent control of the composition of the source gas and the other growth parameters resulting in highly homogeneous film. Moreover, since MOCVD can deposit large area films uniformly, high reproducibility and conformal deposition, it is suitable for commercial manufacturing of these materials. The composition of the film can be easily controlled by the input gas composition in CVD. This is also expected to be expanded to the preparation of the simple component oxide films from the multi component metal oxide films.

Typically an initial guess as to the composition of a multi component films can be obtained from the measured individual deposition rates of the various components of the proposed system. However, the actual depositing rate of given species will depend on the composition of the previously deposited materials and the partial pressures of the various gas phase source. For example, the Pb/Ti ratio in the case of $PbTiO_3$ film¹⁾ and Bi/Ti ratio in the case of $Bi_4Ti_3O_{12}$ film²⁾ were reported by Okada et al when deposited by MOCVD. Pb/Ti and Bi/Ti ratios in Pb-Ti-O and Bi-Ti-O films were different from the estimated ones from the deposition rates of PbO and TiO_2 , and Bi_2O_3 and TiO_2 films, respectively.

In the present study, Y_2O_3 , ZrO_2 and Y_2O_3 -stabilized ZrO_2 (YSZ) thin films were prepared by MOCVD. The depo-

sition rates and the composition of these films were investigated as functions of the input gas concentrations and the deposition temperature. On the basis of these results, the deposition mechanisms of Y_2O_3 , ZrO_2 and YSZ films were discussed.

II. Experimental

Y_2O_3 , ZrO_2 and YSZ films were prepared by CVD using $Y(C_{11}H_{19}O_2)_3-O_2$, $Zr(O-t-C_4H_9)_4-O_2$ and $Y(C_{11}H_{19}O_2)_3-Zr(O-t-C_4H_9)_4-O_2$ systems, respectively. The CVD apparatus having the vertical cold-wall type reactor was used. Substrates used in this study were Al_2O_3 [(102) plane], MgO [(100) plane], SiO_2 layers prepared on (100) silicon wafers, and fused silica. The total gas pressure was maintained at 1.3 kPa and the O_2 partial pressure was maintained at 670 Pa in all cases. The partial pressures of the various source gases were controlled through the vaporizer temperature (T_v), the vaporizer pressure (P_v), and the carrier gas flow rates (l). The source gas concentration, R [source], is known to describe as follows.

$$R[\text{source}] = \frac{P_i(T_v) \cdot l}{P_v} \quad (1)$$

The deposition rate of the film prepared by this study was determined by the substrate weight gain and/or by the X-ray fluorescence intensity of the deposition film. The compo-

sition of the films was determined by XRF(X-ray fluorescence) and ICP(ion coupling plasma).

III. Results and Discussion

3.1. Deposition rates of Y_2O_3 and ZrO_2 component in YSZ film

Fig. 1 shows the XRF intensities of (a) $YL\alpha$ and (b) $ZrK\alpha$ as functions of the calculated deposition weights of Y_2O_3 and ZrO_2 components in YSZ film, respectively. The deposition weights were calculated from the total weight gain of the film and the film composition measured by ICP. The results of un-mixed Y_2O_3 and ZrO_2 films are also shown in Fig. 1. When the deposition weights of Y_2O_3 and ZrO_2 components increased, the intensities increased linearly. These lines were also applied to the un-mixed Y_2O_3 and ZrO_2 films as shown in Fig. 1. Therefore, the deposition weights of Y_2O_3 and ZrO_2 components in YSZ film can be estimated from the intensities of XRF.

3.2. Effect of the input gas concentration

Fig. 2 shows the deposition rates of Y_2O_3 and ZrO_2 films as functions of $R[Y(C_{11}H_{19}O_2)_3]$ and $R[Zr(O-t-C_4H_9)_4]$, respectively at the deposition temperature of 600°C. The substrate

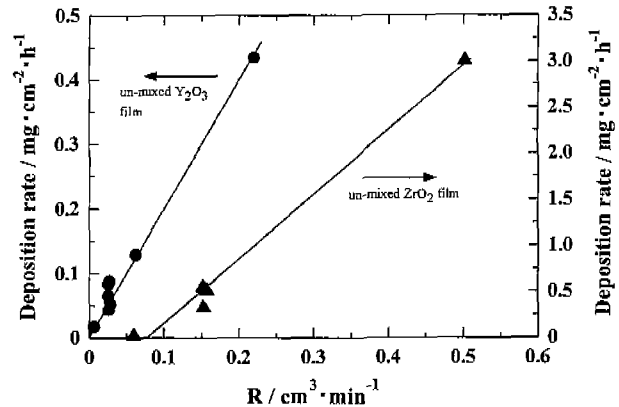


Fig. 2. The deposition rates of un-mixed Y_2O_3 and ZrO_2 films as a function of $R[Y(C_{11}H_{19}O_2)_3]$ and $R[Zr(O-t-C_4H_9)_4]$, respectively at the deposition temperature of 600°C.

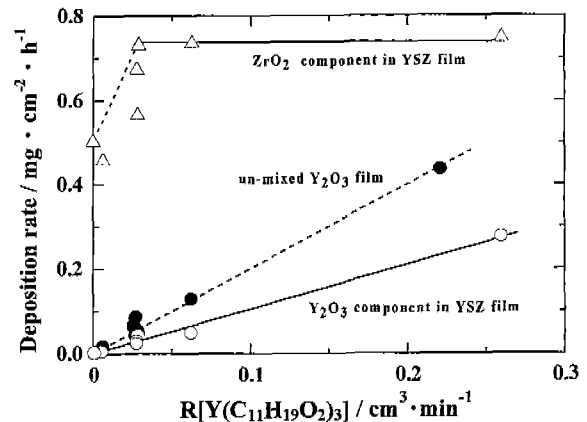


Fig. 3. The deposition rates of Y_2O_3 and ZrO_2 components in YSZ thin film as a function of $R[Y(C_{11}H_{19}O_2)_3]$ under the $R[Zr(O-t-C_4H_9)_4]$ of 0.15 cm^3/min . The deposition rates of un-mixed Y_2O_3 thin film is also shown as dashed line. Deposition temperature was 600°C.

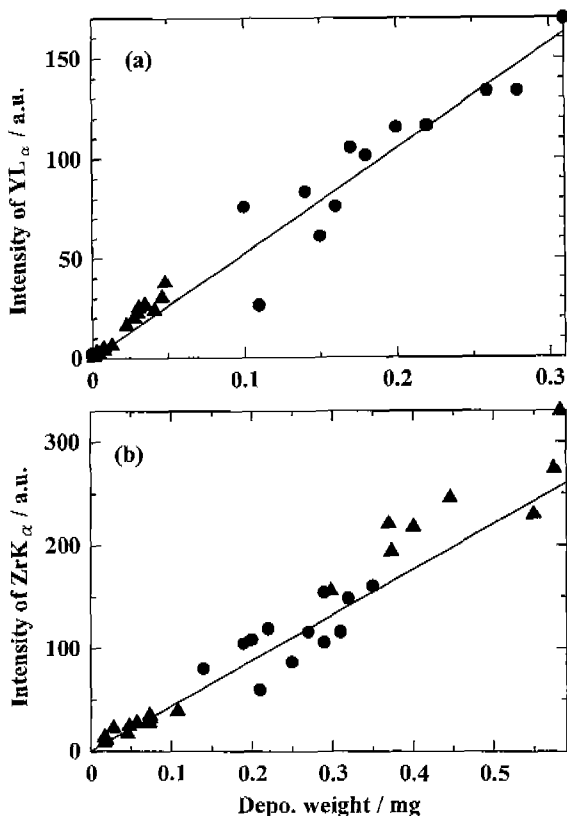


Fig. 1. XRF intensities of (a) $YL\alpha$ and (b) $ZrK\alpha$ as a function of the calculated deposition weights of Y_2O_3 and ZrO_2 components in YSZ film, respectively. The data of un-mixed Y_2O_3 and ZrO_2 films are also added. (a): (●) un-mixed Y_2O_3 film, (▲) Y_2O_3 component in YSZ film and (b): (▲) un-mixed ZrO_2 film, (●) ZrO_2 component in YSZ film.

was a fused silica in this case. When $R[Y(C_{11}H_{19}O_2)_3]$ and $R[Zr(O-t-C_4H_9)_4]$ were increased, the deposition rates of either the Y_2O_3 or ZrO_2 films increased linearly. Therefore, under these conditions, the deposition rates of Y_2O_3 and ZrO_2 thin films are supply limited.

Fig. 3 shows the deposition rates of Y_2O_3 and ZrO_2 components in YSZ thin film as a function of $R[Y(C_{11}H_{19}O_2)_3]$ under the fixed $R[Zr(O-t-C_4H_9)_4]$. The deposition rate of Y_2O_3 film as a function of $R[Y(C_{11}H_{19}O_2)_3]$ seen in Fig. 2 is also shown in Fig. 3 by a dashed line (this case corresponds to 0 cm^3/min of $R[Zr(O-t-C_4H_9)_4]$). The Y_2O_3 component in YSZ thin film linearly increased with increasing $R[Y(C_{11}H_{19}O_2)_3]$. This linearly increased with $R[Y(C_{11}H_{19}O_2)_3]$ for the case of Y_2O_3 component of YSZ film is almost the same as that of the un-mixed Y_2O_3 film. However, the increased of Y_2O_3 component in the YSZ film was smaller than that expected one based on the deposition rate of un-mixed Y_2O_3 films prepared at the same $R[Y(C_{11}H_{19}O_2)_3]$ value. On the other hand, the ZrO_2 component in YSZ film was larger than that expected based on the deposition rate of the ZrO_2 film (when 0

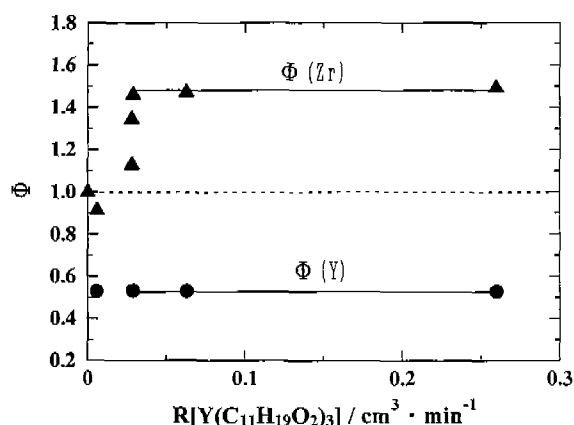


Fig. 4. $\Phi(Y)$ and $\Phi(Zr)$ as a function of $R[Y(C_{11}H_{19}O_2)_3]$ replotted the data shown in Fig. 3. Dashed line shows the line when $\Phi(Y)$ and $\Phi(Zr)$ are unity.

cm^3/min of $R[Y(C_{11}H_{19}O_2)_3]$ but was not depend on $R[Y(C_{11}H_{19}O_2)_3]$. From this figure, the ratios of the deposition rate of Y_2O_3 component in YSZ film to that of un-mixed Y_2O_3 film is found to be independent of $R[Y(C_{11}H_{19}O_2)_3]$. The same result is also expected by the ratio of that of ZrO_2 component in YSZ film to that of un-mixed ZrO_2 film. Therefore, we define the following deposition efficiency of Y and Zr atoms, $\Phi(Y)$ and $\Phi(Zr)$, at the fixed $R[Y(C_{11}H_{19}O_2)_3]$ and $R[Zr(O-t-C_4H_9)_4]$, respectively:

$$\Phi(Y) = \frac{\text{Deposition rate of } Y_2O_3 \text{ component in YSZ film}}{\text{Deposition rate of } Y_2O_3 \text{ film}} \quad (2)$$

$$\Phi(Zr) = \frac{\text{Deposition rate of } ZrO_2 \text{ component in YSZ film}}{\text{Deposition rate of } ZrO_2} \quad (3)$$

In this case, $[\Phi(Y)]/[\Phi(Zr)]$ ratio corresponds to the ratio of Y/Zr ratio in YSZ film to that estimated from the deposition rates of un-mixed Y_2O_3 and ZrO_2 films.

Fig. 4 shows $\Phi(Y)$ and $\Phi(Zr)$ as a function $R[Y(C_{11}H_{19}O_2)_3]$ replotted the data shown in Fig. 3. Dashed line shows the line that $\Phi(Y)$ and $\Phi(Zr)$ are unity; the deposition rates of Y_2O_3 and ZrO_2 compositions in YSZ film are the same as those of un-mixed Y_2O_3 and ZrO_2 films, respectively. $\Phi(Y)$ and $\Phi(Zr)$ are almost constant irrespective of $R[Y(C_{11}H_{19}O_2)_3]$ except below $R[Y(C_{11}H_{19}O_2)_3]$ of $0.03 \text{ cm}^3/min$. $\Phi(Zr)$ is above unity and $\Phi(Y)$ is below unity, so that $\Phi(Y)/\Phi(Zr)$ ratio is below unity.

Fig. 5 shows the logarithm of the Y/Zr ratio in YSZ films as a function of the Y/Zr ratio estimated from the deposition rates of un-mixed Y_2O_3 and ZrO_2 films under the same $R[Y(C_{11}H_{19}O_2)_3]$ and $R[Zr(O-t-C_4H_9)_4]$. The Y/Zr ratio in YSZ film increased linearly with that estimated from the deposition rates of un-mixed Y_2O_3 and ZrO_2 films. This is because $\Phi(Y)$ and $\Phi(Zr)$ are irrespective of the $R[Y(C_{11}H_{19}O_2)_3]/R[Zr(O-t-C_4H_9)_4]$ ratio. However, the Y/Zr ratio in YSZ film

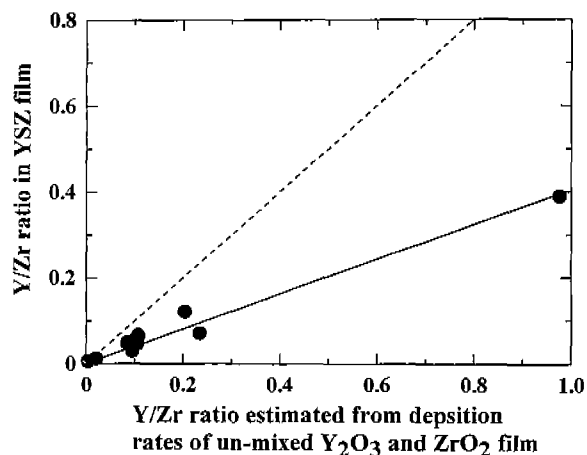


Fig. 5. The Y/Zr ratio in YSZ films as a function of the Y/Zr ratio estimated from the deposition rates of un-mixed Y_2O_3 and ZrO_2 films under the same $R[Y(C_{11}H_{19}O_2)_3]$ and $R[Zr(O-t-C_4H_9)_4]$. Dashed line shows that both of two Y/Zr ratios are equal.

is smaller than the estimated Y/Zr ratio. This result appears to be related to composition dependent surface kinetics or due to the differences of the chemical potential of the various film constituents. The slope in Fig. 5 corresponds to the ratio of $\Phi(Y)$ to $\Phi(Zr)$, $[\Phi(Y)]/[\Phi(Zr)]$. This result indicates that the $[\Phi(Y)]/[\Phi(Zr)]$ ratio is constant irrespective of $R[Y(C_{11}H_{19}O_2)_3]$ and $R[Zr(O-t-C_4H_9)_4]$. Therefore, the Y/Zr ratio in YSZ film can be controlled precisely by the $[\Phi(Y)]/[\Phi(Zr)]$ ratio. This means that Y/Zr ratio in YSZ film can be controlled by the ratio of $R[Y(C_{11}H_{19}O_2)_3]$ to $R[Zr(O-t-C_4H_9)_4]$, because the deposition rates of un-mixed Y_2O_3 and ZrO_2 films increased linearly with $R[Y(C_{11}H_{19}O_2)_3]$ and $R[Zr(O-t-C_4H_9)_4]$ as shown in Fig. 2. In fact, the YSZ film with the Y/Zr ratio from 0.004 to 0.4 can be deposited successfully by changing the $R[Y(C_{11}H_{19}O_2)_3]/R[Zr(O-t-C_4H_9)_4]$ ratio.

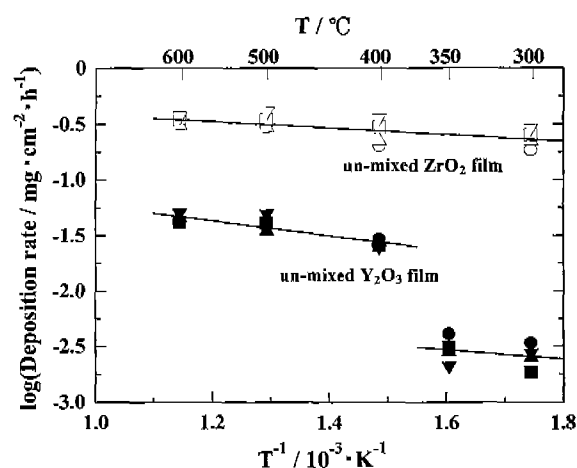


Fig. 6. The logarithms of the deposition rates of un-mixed Y_2O_3 and un-mixed ZrO_2 thin films as a function of the reciprocal of the deposition temperature. $R[Y(C_{11}H_{19}O_2)_3]$: $0.027 \text{ cm}^3/min$, $R[Zr(O-t-C_4H_9)_4]$: $0.15 \text{ cm}^3/min$. (\circ , \bullet): (102) Al_2O_3 , (\triangle , \blacktriangle): (100) MgO , (\square , \blacksquare): $SiO_2/(100) \text{ Si}$, (∇ , \blacktriangledown): fused silica.

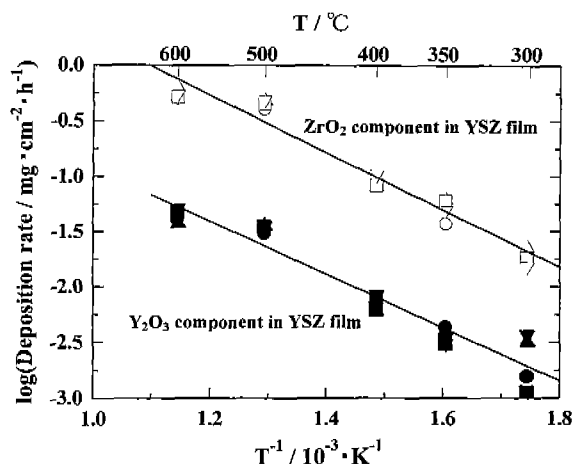


Fig. 7. The logarithms of the deposition rates of Y_2O_3 and ZrO_2 components of YSZ thin film as a function of the reciprocal of the deposition temperature. $R[\text{R}(\text{C}_{11}\text{H}_{19}\text{O}_2)_3]$: $0.027 \text{ cm}^3/\text{min}$, $R[\text{Zr}(\text{O}-t-\text{C}_4\text{H}_9)_4]$: $0.15 \text{ cm}^3/\text{min}$. (\circ \bullet): (102) Al_2O_3 , (\triangle \blacktriangle): (100) MgO , (\square \blacksquare): SiO_2 (100) Si , (∇ \blacktriangledown): fused silica.

3.3. Effect of deposition temperature

Figs 6 and 7 show the logarithm of deposition rates of Y_2O_3 and ZrO_2 thin films and Y_2O_3 and ZrO_2 components of YSZ thin film, respectively as a function of the reciprocal of the deposition temperature. The various substrate exhibited similar behavior. From Fig. 6, the deposition rates of the ZrO_2 thin film exhibited Arrhenius behavior between 300 and 600°C. On the other hand, the Y_2O_3 thin films exhibited Arrhenius behavior between 400 and 600°C, but the deposition temperature dependency below 350°C was different from that above 400°C. On the other hand, as shown in Fig. 7, Y_2O_3 and ZrO_2 components in YSZ film show Arrhenius relations from 300 to 600°C. Moreover, these slopes were almost the same. This means that the activation energies, E_a , of these components in YSZ film are almost the same and are calculated to be about 48 kJ/mol from the slope of the lines in Fig. 7. This value is 4 and 8 times larger than when these of un-mixed Y_2O_3 and ZrO_2 films, respectively (13 kJ/mol for Y_2O_3 film from 400 to 600°C and 6 kJ/mol for ZrO_2 film from 300 to 600°C). This result indicates that rate-determining deposition for YSZ films is different from those of un-mixed Y_2O_3 and ZrO_2 films. Moreover the deposition rate-determining steps or the equilibrium chemicals of Y_2O_3 and ZrO_2 components in YSZ films are considered to be different from those of un-mixed Y_2O_3 and ZrO_2 thin films. As a result, the Y/Zr ratio in YSZ thin films cannot be estimated from the deposition rates of un-mixed Y_2O_3 and ZrO_2 films. These results facilitate the preparation of multi component metal oxide film. The E_a of the YSZ thin films of the present study is similar to the reported one by G. Garica *et al.*⁹ for YSZ film prepared from $\text{Y}(\text{C}_{11}\text{H}_{19}\text{O}_2)_3\text{-Zr}(\text{O}-t-\text{C}_4\text{H}_9)_4\text{-O}_2$ system. E_a of ZrO_2 thin film

prepared by this study is similar to that reported by Itoh *et al.*⁴ from the $\text{Zr}(\text{O}-t-\text{C}_4\text{H}_9)_4\text{-O}_2$ system. However, the E_a of the present study is one of the smallest among reported values. Also, E_a of the Y_2O_3 film prepared in this study is less than one-tenth of that reported by Akiyama *et al.*⁵ However, the comparison of E_a of YSZ thin film with those of un-mixed Y_2O_3 or ZrO_2 thin films has not been previously detailed. Therefore, the clear difference of E_a for YSZ thin film deposition with those of un-mixed Y_2O_3 and ZrO_2 thin films has not been previously reported.

IV. Conclusion

Y_2O_3 , ZrO_2 and YSZ thin films were prepared by MOCVD. The effects of the input gas concentration and the deposition temperature on the deposition rate were investigated. As a result, the following results were obtained.

(1) The deposition rates of Y_2O_3 and ZrO_2 films at 600°C appear to be determined by the input gas concentrations.

(2) The Y/Zr ratio in the YSZ film could be controlled by the relative input gas concentration ratio. This is because the ratios of the deposition rates of Y and Zr atoms in Y_2O_3 and ZrO_2 films to those in YSZ films, Φ , are constant irrespective of the input gas concentration. However, the Y/Zr ratio in YSZ thin film was lower than that estimated from the deposition rates of un-mixed Y_2O_3 and ZrO_2 films. This is because the Φ of Y and Zr atoms are not equal.

(3) The activation energies of both Y_2O_3 and ZrO_2 components in YSZ thin film were similar but were more than 4 times larger than those of either un-mixed Y_2O_3 and ZrO_2 thin films. Therefore, the rate-determining steps of YSZ thin film are considered to be different from those of Y_2O_3 and ZrO_2 films.

Reference

1. M. Okada, H. Watanabe, M. Murakami, A. Nishiwaki and K. Tomomi, "Preparation of PbTiO_3 Thin Films by MOCVD under Atmospheric Pressure," *J. Ceram. Soc. Jpn.*, **96**(6), 687-693 (1988).
2. M. Miyajima, R. Muhammet and M. Okada, "Preparation and Electric Properties of Ferroelectric $\text{Bi}_4\text{Ti}_3\text{O}_{12}$ Thin Films by MOCVD," *Nihon Kagaku Kai-shi*, **10**, 1373-1378 (1991).
3. G. Carcia, J. Casado, J. Libre, J. Cifre, A. Figueras, S. Gali and J. Bassas, "Structural Properties of Yittri-Stabilized Zirconia Films Grows on Silicon(001) Using MOCVD," *Chem. Vapor Dep.*, **3**, 91-96 (1997).
4. H. Itoh, T. Tanaka, Y. Suzuki and K. Sugiyama, "Preparation of ZrO_2 - MgO Thin Films by MOCVD," *J. Ceram. Soc. Jpn.*, **97**, 1077-1081 (1989).
5. Y. Akiyama, T. Sato and N. Imaishi, "Reaction Analysis for ZrO_2 and Y_2O_3 Thin Films Grown by Low-Pressure Metalorganic Chemical Vapor Deposition Using β -diketonate Complex," *J. Cryst. Growth*, **147**, 130-146 (1995).